

- Schiff base complex shows that Wat²¹ is equivalent to Wat²⁹. Also in the native structure, a water molecule is found in the identical position (within 0.5 Å of Wat²⁹ of the carbinolamine). Wat⁷² in the Schiff base complex could correspond to the water molecule derived from protonation of the hydroxyl group of the carbinolamine.
25. Known class I structures used for comparison were KDPG aldolase in complex with pyruvate [Protein Data Bank (PDB) code 1EUA] (17), human muscle fructose 1,6-bisphosphate aldolase (PDB code 4ALD) (19), rabbit muscle 1,6-bisphosphate fructose aldolase (PDB code 1ADO) (20), and transaldolase B (PDB code 1UCW) (21).
 26. This mutant crystallized under the same conditions as the wild type, and the substrate soak was repeated as reported in Table 1.
 27. This observation was also made for the rabbit aldolase A, where the Lys¹⁴⁶ → Arg¹⁴⁶ mutant retained the ability to form the Schiff base intermediate (43).
 28. F. H. Westheimer, D. E. Schmidt Jr., *Biochemistry* **10**, 1249 (1971).
 29. F. H. Westheimer, *Tetrahedron* **51**, 3 (1995).
 30. Experimental conditions for the pH activity profile were as follows: 25 mM buffer solutions of sodium formate (pH 3.5, 3.0, and 4.0); sodium acetate (pH 4.5, 5.0, and 5.5); MES (pH 5.5, 6.0, and 6.5); MOPS (pH 6.5, 7.0, and 7.5); tetraethylammonium-chloride (TEA-HCl) (pH 7.5, 8.0, and 8.5); CAPSO (pH 8.5, 9.0, and 9.5), and CAPS (pH 10, 10.5, and 11.0). V_{max} was measured from pH 4 to 10 in the retroaldol direction with 3 mM DRP in 50 mM (pH 7.5) TEA-HCl buffer in the presence of 0.3 mM reduced nicotinamide adenine dinucleotide (NADH) using a glyceraldehyde 3-phosphate dehydrogenase/triisophosphate isomerase (GPD/TPI)-coupled (5.3 U/ml, Sigma G-1881) enzyme system at 25°C by observing the rate of decrease of NADH concentration as monitored at 340 nm (44).
 31. In rabbit aldolase A, the equivalent Lys¹⁴⁶ residue has been implicated as being involved in cleavage and condensation of the C3–C4 bond of fructose 1,6-bisphosphate (45), in addition to lowering the pK_a of Lys²²⁹.
 32. All solvent-accessible surface areas were calculated with the program MS (46) with a 1.4 Å probe sphere and standard atomic radii (47).
 33. Experimental conditions for the Schiff base trapping experiment were as follows: DERA (1 mg/ml) was incubated with 5 mM acetaldehyde in 20 mM TEA-HCl, 50 mM NaCl, and 2 mM CaCl₂ (pH 7.4) at 22°C for 10 min. Fifty mM NaBH₄ was added, and incubation continued for 12 hours. Samples were dialyzed against dH₂O and then purified by high-performance liquid chromatography on a C18 column before analysis by electrospray ionization mass spectrometry (with a Perkin Elmer API III Sciex triple quadrupole). Observed masses agreed within ±4 daltons to theoretical values.
 34. A. Heine, J. G. Luz, C.-H. Wong, I. A. Wilson, in preparation.
 35. J. A. Littlechild, H. C. Watson, *Trends Biochem. Sci.* **18**, 36 (1993).
 36. The activity of the class I aldolase from halophilic archaeobacterium *Haloarcula vallismortis* was not affected by carboxypeptidase digestion (48).
 37. The model was constructed with Molecular Simulations Insight 2000. Setup was as described (49). The CVFF force field provided in the Discover module of InsightII was used.
 38. C. F. Barbas III, thesis, Texas A&M University, College Station, TX (1989).
 39. Experimental conditions for deuteropropanal synthesis and the DERA exchange experiment were as follows: (R)-2-deuteropropanal was synthesized from (S)-(+)-1,2-propanediol as described in (50) with minor modification. ¹H NMR (CDCl₃, 500 MHz): 3.62 (d, J = 6.97 Hz, 2H), 1.60 to 1.55 (m, 1H), 0.91 (d, J = 7.34 Hz, 3H). ¹³C NMR (CDCl₃, 125 MHz): 64.58, 24.79 (t, J = 20 Hz), 9.91. (R)-2-deuteropropanal: [α]_D = +1.11°, (CDCl₃, c = 0.18); lit. +0.06°, (neat). (S)-2-deuteropropanal was prepared analogously: [α]_D = -0.05° (CDCl₃, c = 1.8); lit. -0.06° (neat). In an NMR tube, (R)- or (S)-2-deuteropropanal was incubated at 0.4 mM in 100 mM TEA-HCl buffer made up with D₂O together with 8 mM pyruvic acid, 1 mM NAD⁺, yeast alcohol dehydrogenase (0.25 mg/ml) (82.5 U), and L-lactic dehydrogenase (0.25 mg/ml) (214.5 U), pH in D₂O (pD) = 7.1. After the oxidation of deuteropropanol to deuteropropanal was deemed substantially complete by the appearance of the aldehyde C3 resonance by ¹H NMR (D₂O, 500 MHz): 1.08 (d, J = 7.34 Hz, 3H), then 0.5 mg/ml (50 U) wild-type DERA was added. For (R)-2-deuteropropanal, this resonance collapses to a singlet 1.04 (s, 3H) after 3 hours, whereas for (S)-2-deuteropropanal it remains unchanged.
 40. L. Chen, D. P. Dumas, C.-H. Wong, *J. Am. Chem. Soc.* **114**, 741 (1992).
 41. T. M. Larsen, M. M. Benning, I. Rayment, G. H. Reed, *Biochemistry* **37**, 6247 (1998).
 42. R. R. Copley, G. J. Barton, *J. Mol. Biol.* **242**, 321 (1994).
 43. A. J. Morris, R. C. Davenport, D. R. Tolan, *Prot. Eng.* **9**, 61 (1996).
 44. P. C. Nicholas, *Biochem. Soc. Trans.* **16**, 752 (1988).
 45. A. J. Morris, D. R. Tolan, *Biochemistry* **33**, 12291 (1994).
 46. M. L. Connolly, *J. Appl. Crystallogr.* **16**, 439 (1983).
 47. S. Sheriff, *Immunomethods* **3**, 191 (1993).
 48. G. Krishnan, W. Altekar, *Eur. J. Biochem.* **195**, 343 (1991).
 49. G. DeSantis, J. B. Jones, *J. Am. Chem. Soc.* **120**, 8582 (1998).
 50. M. M. Green, J. M. Moldovan, J. G. McGrew II, *J. Org. Chem.* **39**, 2166 (1974).
 51. Z. Otwinowski, W. Minor, *Methods Enzymol.* **276A**, 307 (1997).
 52. A. T. Brünger et al., *Acta Crystallogr. D* **54**, 905 (1998).
 53. G. M. Sheldrick, T. R. Schneider, *Methods Enzymol.* **277B**, 319 (1997).
 54. T. A. Jones, J. Y. Zou, S. W. Cowan, M. Kjeldgaard, *Acta Crystallogr. A* **47**, 110 (1991).
 55. H. Kim, U. Certa, H. Döbeli, P. Jakob, W. G. Hol, *Biochemistry* **37**, 4388 (1998).
 56. J. Sygusch, D. Beaudry, M. Allaire, *Proc. Natl. Acad. Sci. U.S.A.* **84**, 7846 (1987).
 57. R. A. Laskowski, M. W. MacArthur, D. S. Moss, J. M. Thornton, *J. Appl. Crystallogr.* **26**, 283 (1993).
 58. P. C. Nicholas, *Biochem. Soc. Trans.* **16**, 752 (1988).
 59. Experimental conditions for propanal exchange with DERA mutants were as follows: In an NMR tube, propanal was incubated at 200 mM in 100 mM TEA-HCl buffer made up with D₂O (pD = 7.1) and DERA (2 mg/ml) was added (50 U for wild-type DERA). Samples were analyzed by ¹H NMR (D₂O, 250 MHz). For wild-type DERA, the C3-aldehyde triplet resonance 1.03 (t, J = 7.01 Hz, 3H) collapses to a doublet 1.02 (d, J = 7.3 Hz, 3H).
 60. P. J. Kraulis, *J. Appl. Crystallogr.* **24**, 946 (1991).
 61. E. A. Merritt, D. J. Bacon, *Methods Enzymol.* **277**, 505 (1997).
 62. We gratefully acknowledge helpful discussions with F. Huang, S. Fong, L. Lee, T. Tolbert, P. Sears, W. W. Cleland, G. M. Sheldrick, J. H. Naismith, and R. A. Lerner. Supported by NIH grants GM44154 (C.H.W.) and CA27489 (I.A.W.), a Natural Science and Engineering Research Council of Canada postdoctoral fellowship (G.D.), and a UNCF-Merck Science Initiative fellowship (M.M.). We thank the Stanford Synchrotron Radiation Laboratory staff of beamline 9-2, X. Dai, and S. E. Greasley for help with data collection and processing, and M. Elsliger for computational assistance. This is publication 14200-MB from the Scripps Research Institute. The coordinates have been deposited in the PDB with access codes 1JCL (wild-type DERA) and 1JCJ (K201L mutant of DERA) and are available immediately from aheine@scripps.edu.

19 June 2001; accepted 2 August 2001

Carboxyl-Terminal Modulator Protein (CTMP), a Negative Regulator of PKB/Akt and v-Akt at the Plasma Membrane

Sauveur-Michel Maira,¹ Ivana Galetic,¹ Derek P. Brazil,¹ Stefanie Kaech,^{1*} Evan Ingley,^{1†} Marcus Thelen,² Brian A. Hemmings^{1‡}

The PKB (protein kinase B, also called Akt) family of protein kinases plays a key role in insulin signaling, cellular survival, and transformation. PKB is activated by phosphorylation on residues threonine 308, by the protein kinase PDK1, and Serine 473, by a putative serine 473 kinase. Several protein binding partners for PKB have been identified. Here, we describe a protein partner for PKB α termed CTMP, or carboxyl-terminal modulator protein, that binds specifically to the carboxyl-terminal regulatory domain of PKB α at the plasma membrane. Binding of CTMP reduces the activity of PKB α by inhibiting phosphorylation on serine 473 and threonine 308. Moreover, CTMP expression reverts the phenotype of v-Akt-transformed cells examined under a number of criteria including cell morphology, growth rate, and in vivo tumorigenesis. These findings identify CTMP as a negative regulatory component of the pathway controlling PKB activity.

PKB is a major downstream target of receptor tyrosine kinases that signal via the phosphatidylinositol 3-kinase (PI 3-kinase). PKB mediates a wide variety of biological responses to insulin and insulin-like growth factor 1

(IGF-1) and other growth factors (1–2). Upon cell stimulation, the kinase is translocated to the plasma membrane, where it is phosphorylated on two amino acids, Thr³⁰⁸ in the catalytic domain and Ser⁴⁷³ in the COOH-

REPORTS

Fig. 2. Interaction of CTMP and PKB α in quiescent cells, and phosphorylation following stimulation. (A) Schematic diagram of recombinant proteins used in these experiments (33). (B) COS-1 cells were transfected with 7.5 μ g of the indicated PKB expression vectors, lysed, and fractionated (37). Soluble (S100) and particulate (P100) fractions were analyzed by Western blotting using the HA mAb 12CA5 (14). (C) COS-1 cells were transfected with 7.5 μ g of the indicated PKB (33) and CTMP (29) expression vectors. After serum starvation (24 hours) and stimulation with 100 μ M pervanadate (15 min at 37°C, +Per.), cells were lysed and fractionated. Immunoprecipitations were performed from S100 and P100 fractions using an antibody against Flag (14). PKB α expression was analyzed using an HA antibody (upper panel), CTMP expression was analyzed using Flag anti-serum (middle panel), and CTMP-bound PKB α was detected using an HA antibody (bottom panel). The asterisk represents the IgG heavy chain. (D) COS-1 cells were transfected with 7.5 μ g of pF-CTMP and with pGST or pGST-PKB-RD. Cells were lysed and fractionated as in Fig. 2B, and immunoprecipitations were performed from the S100 fractions with a Flag antibody. Association of GST-PKB-RD with CTMP was analyzed using a GST antibody (14). (E) Cells stably expressing Flag-CTMP were labeled in vivo with [32 P] orthophosphate (34). After immunoprecipitation, phosphorylated Flag-CTMP was revealed by SDS-polyacrylamide gel electrophoresis (SDS-PAGE) and Western-blotting, followed by autoradiography of the membrane (bottom panel). Expression level of Flag-CTMP was revealed by immunoblotting of the membrane with antibody against Flag (upper panel).

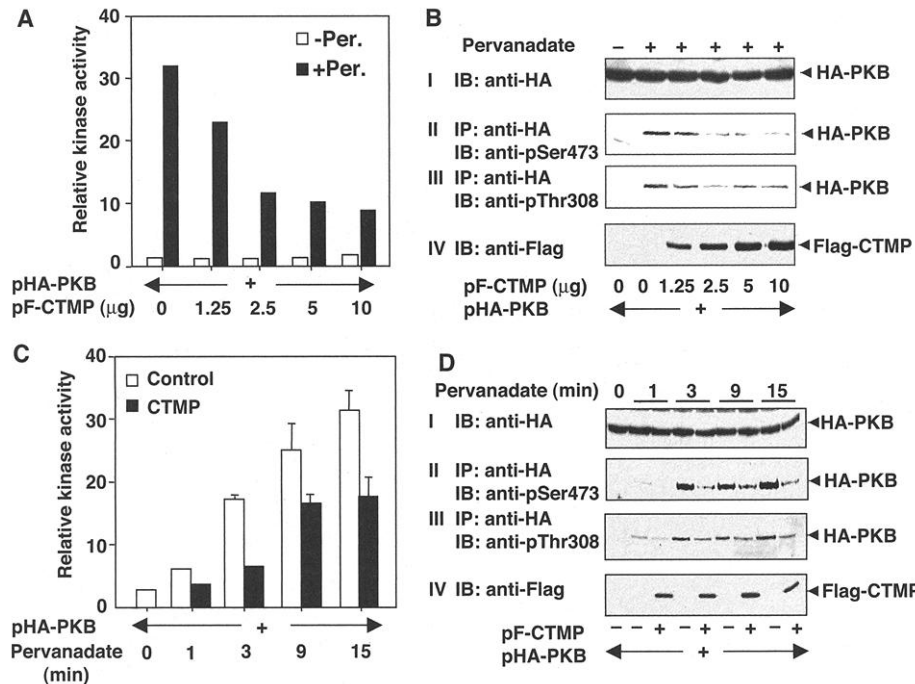
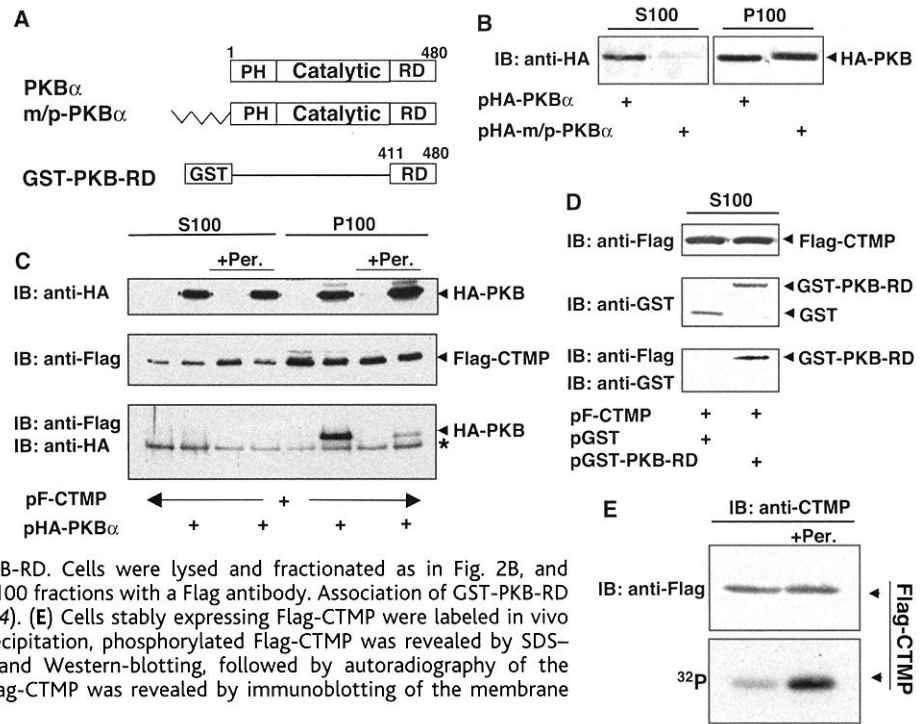


Fig. 3. CTMP inhibits PKB α activity by preventing its phosphorylation by upstream kinases. (A) COS-1 cells were cotransfected with an HA-PKB expression vector (2.5 μ g) and with the indicated amount of pF-CTMP. Cells were serum-starved (24 hours), and stimulated with vehicle control (white bars) or 100 μ M pervanadate (black bars) for 10 min at 37°C. Cells were then lysed and analyzed for PKB kinase activity as described (35). (B) The phosphorylation status of PKB α was investigated by using antibodies against pSer 473 (panel II) and Thr 308 (panel III) (14). Expressed PKB α (panel I) and CTMP (panel IV) proteins were detected with the indicated antibodies (14). (C) COS-1 cells were transfected with an HA-PKB α expression vector (2.5 μ g) together with 5 μ g control vector (control, white bars) or 5 μ g pF-CTMP (CTMP, black bars). Serum-starved cells (24 hours) were then stimulated with 100 μ M pervanadate at 37°C for the indicated times, lysed, and processed for immune-kinase assay (35). (D) Immunoprecipitations from COS-1 cells transfected with the indicated constructs were analyzed for phosphorylation on PKB α residues Ser 473 or Thr 308 as described in Fig. 3B.

two forms of CTMP exist in these cells (Fig. 1, C and F; also see Fig. 5 for details). Transfection of CTMP without an epitope tag also produced two species of CTMP, suggesting that this protein undergoes posttranslational modifications such as phosphorylation in cells (Fig. 1F; also see Fig. 2E). It is interesting that the lower of the two CTMP forms in transfected cells comigrated with endogenous CTMP detected in the P100 fraction of LN229 cells (Fig. 1D). This further suggests that CTMP localization in the cell may be regulated by posttranslational modifications such as phosphorylation.

To further explore the biological relevance of the PKB α -CTMP complex, this interaction was analyzed in mammalian cells by immunoprecipitation. In cell extracts from transfected COS-1 cells lysed in buffer containing 1% NP-40 (v/v), CTMP formed a complex with a COOH-terminal regulatory domain mutant of PKB α (GST-PKB-RD, Fig. 2A), but not with full-length PKB α . One interpretation of this result is that binding of CTMP and PKB α may require intact plasma membrane structures, because both proteins have the ability to localize at the plasma membrane [(17) and Fig. 1B]. We therefore lysed transfected COS-1 cells in HEPES/sucrose buffer, facilitating the preparation of cytosolic (S100) and membrane (P100) fractions for immunoprecipitation. The efficiency of the fractionation was confirmed by transfection of a membrane-targeted PKB (m/p-PKB), a construct containing sites for myristoylation and palmitoylation of PKB that result in constitutive membrane anchoring [(17) and Fig. 2A]. The m/p-PKB protein was exclusively localized in the P100 fraction of lysed COS-1 cells (Fig. 2B). In contrast, wild-type PKB α

REPORTS

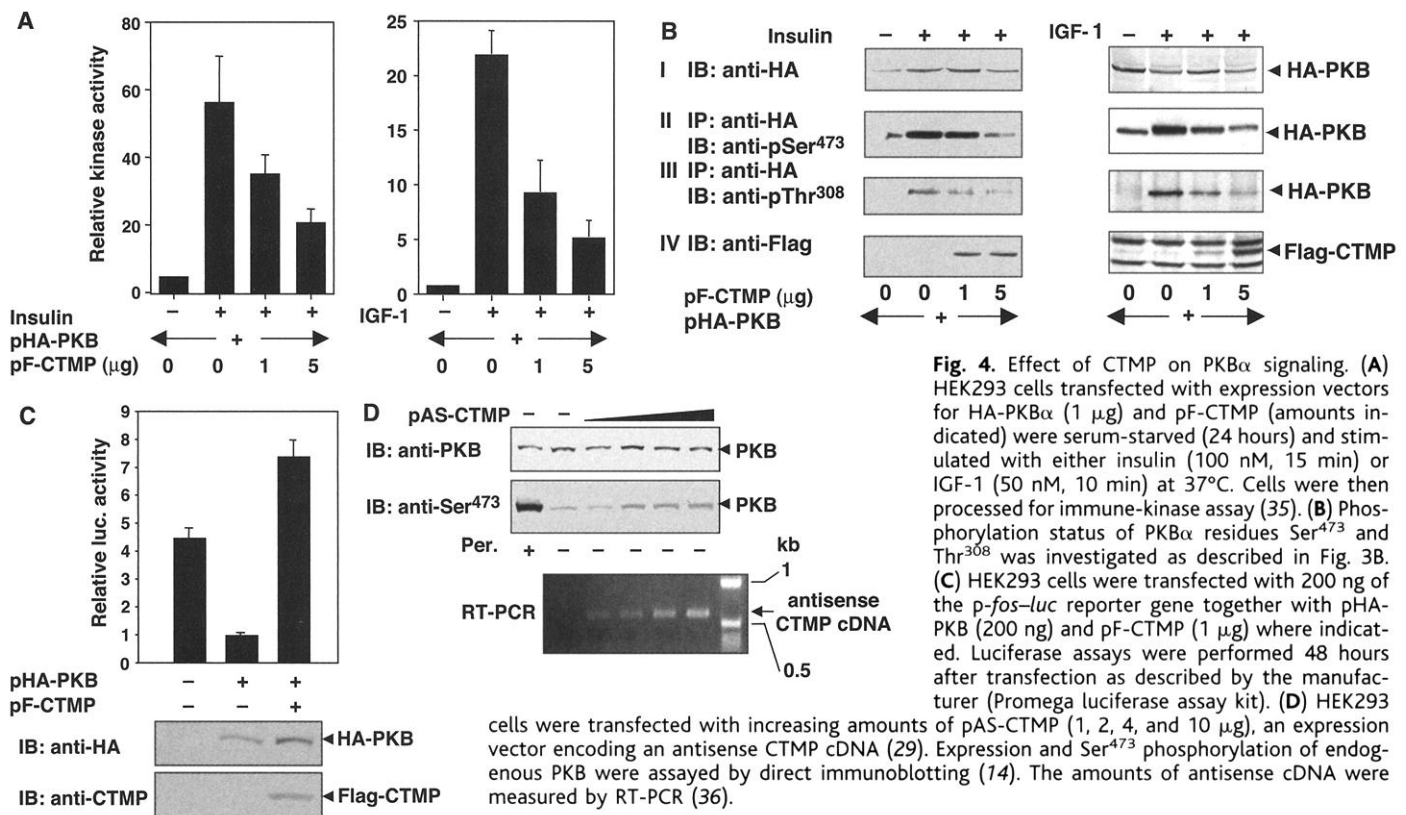


Fig. 4. Effect of CTMP on PKB α signaling. (A) HEK293 cells transfected with expression vectors for HA-PKB α (1 μ g) and pF-CTMP (amounts indicated) were serum-starved (24 hours) and stimulated with either insulin (100 nM, 15 min) or IGF-1 (50 nM, 10 min) at 37°C. Cells were then processed for immune-kinase assay (35). (B) Phosphorylation status of PKB α residues Ser⁴⁷³ and Thr³⁰⁸ was investigated as described in Fig. 3B. (C) HEK293 cells were transfected with 200 ng of the *p-fos-luc* reporter gene together with pHA-PKB (200 ng) and pF-CTMP (1 μ g) where indicated. Luciferase assays were performed 48 hours after transfection as described by the manufacturer (Promega luciferase assay kit). (D) HEK293 cells were transfected with increasing amounts of pAS-CTMP (1, 2, 4, and 10 μ g), an expression vector encoding an antisense CTMP cDNA (29). Expression and Ser⁴⁷³ phosphorylation of endogenous PKB were assayed by direct immunoblotting (14). The amounts of antisense cDNA were measured by RT-PCR (36).

was equally distributed between the membrane and cytosolic fractions. Association of PKB α and CTMP was examined by cotransfection of COS-1 cells with constructs encoding epitope-tagged versions of both proteins [hemagglutinin-tagged (HA)-PKB α and Flag-CTMP, Fig. 2C]. Both PKB α (upper panel) and CTMP (middle panel) were detected in cytosolic (S100) and membrane (P100) fractions (Fig. 2C). In addition, PKB α was observed in CTMP immunoprecipitates from membrane, but not cytosolic fractions (Fig. 2C, bottom panel). Treatment of COS-1 cells with pervanadate, an inhibitor of protein tyrosine phosphatases that potently activates PKB (18), disrupted the PKB α -CTMP interaction in the membrane fraction (Fig. 2C, bottom panel). These data confirm that PKB α interacts with CTMP in quiescent or unstimulated cells and that activation of PKB α with pervanadate perturbs this interaction. In contrast to full-length PKB α , a truncation mutant containing the COOH-terminal regulatory domain of PKB α (GST-PKB-RD, Fig. 2A) was detected in CTMP immunoprecipitates from cytosolic fractions of COS-1 cells (Fig. 2D). These observations suggest that a region of PKB α not present in the GST-PKB-RD construct inhibits the binding of CTMP to cytosolic PKB α . Alternately, other proteins may be involved in the formation of PKB-CTMP complexes. These data further support the hypothesis that binding of full-length PKB α and CTMP occurs only at the plasma membrane.

To explore a potential mechanism for the inhibitory effect of pervanadate on PKB α -CTMP complexes, we monitored phosphorylation of CTMP during PKB activation. In vivo labeling of cells stably expressing Flag-CTMP with [³²P]orthophosphate demonstrated a fourfold increase in CTMP phosphorylation after pervanadate treatment (Fig. 2E), supporting the idea that CTMP is regulated at the posttranslational level by as-yet-unidentified protein kinases.

Activation of PKB α occurs via phosphorylation of Thr³⁰⁸ in the activation loop of the kinase domain and of Ser⁴⁷³ in the COOH-terminal regulatory domain (5). To test the influence of CTMP binding on activation of PKB α , we assayed kinase activity in immune complexes from transfected COS-1 cells treated with pervanadate. Pervanadate-stimulated PKB α activity was decreased in a manner dependent on the amount of transfected CTMP (Fig. 3A). Therefore, CTMP binding appears to have an inhibitory effect on PKB. Increased CTMP expression led to decreased phosphorylation on both Ser⁴⁷³ and Thr³⁰⁸ residues of PKB α , most notably on Ser⁴⁷³ (Fig. 3B). Especially at late time points, kinase activity of PKB α was stimulated by pervanadate, despite the presence of CTMP (Fig. 3C). This increase in activity over time was reflected in increases in phosphorylation of PKB α residues Ser⁴⁷³ and Thr³⁰⁸ in the presence or absence of CTMP (Fig. 3D). These results show that binding of CTMP to PKB α inhibits, but does not completely abol-

ish, pervanadate-stimulated phosphorylation of the key amino acids necessary for kinase activity of PKB α .

To determine the effect of CTMP on PKB α activity in response to physiological stimuli, we treated HEK293 cells transfected with constructs expressing PKB α and various amounts of CTMP with insulin or IGF-1. The kinase activity of PKB α was stimulated by both insulin and IGF-1, and this stimulation was progressively inhibited by increasing amounts of CTMP expression (Fig. 4A). Furthermore, analysis of the phosphorylation status of PKB revealed that CTMP expression led to a decrease in Ser⁴⁷³ and Thr³⁰⁸ phosphorylation induced by insulin and IGF-1 (Fig. 4B). These data reinforce the results seen with pervanadate (Fig. 3) and support the hypothesis that CTMP is an inhibitor of PKB in vivo.

To explore the effect of CTMP on downstream effectors of PKB, we analyzed the consequence of CTMP expression on PKB α -mediated transcriptional regulation. PKB α reduces both basal and serum-stimulated transcriptional activity of the *c-fos* promoter (16). Coexpression of CTMP completely abolished the inhibitory effect of PKB α on *c-fos*-mediated transcription (Fig. 4C), showing that CTMP inhibitory activity is correlated with a reversion of PKB downstream target function. Indeed, CTMP expression increased *c-fos* promoter activity above control levels, possibly through inhibition of endogenous PKB (Fig. 4C). In addition, expression of CTMP reduced phosphoryl-

REPORTS

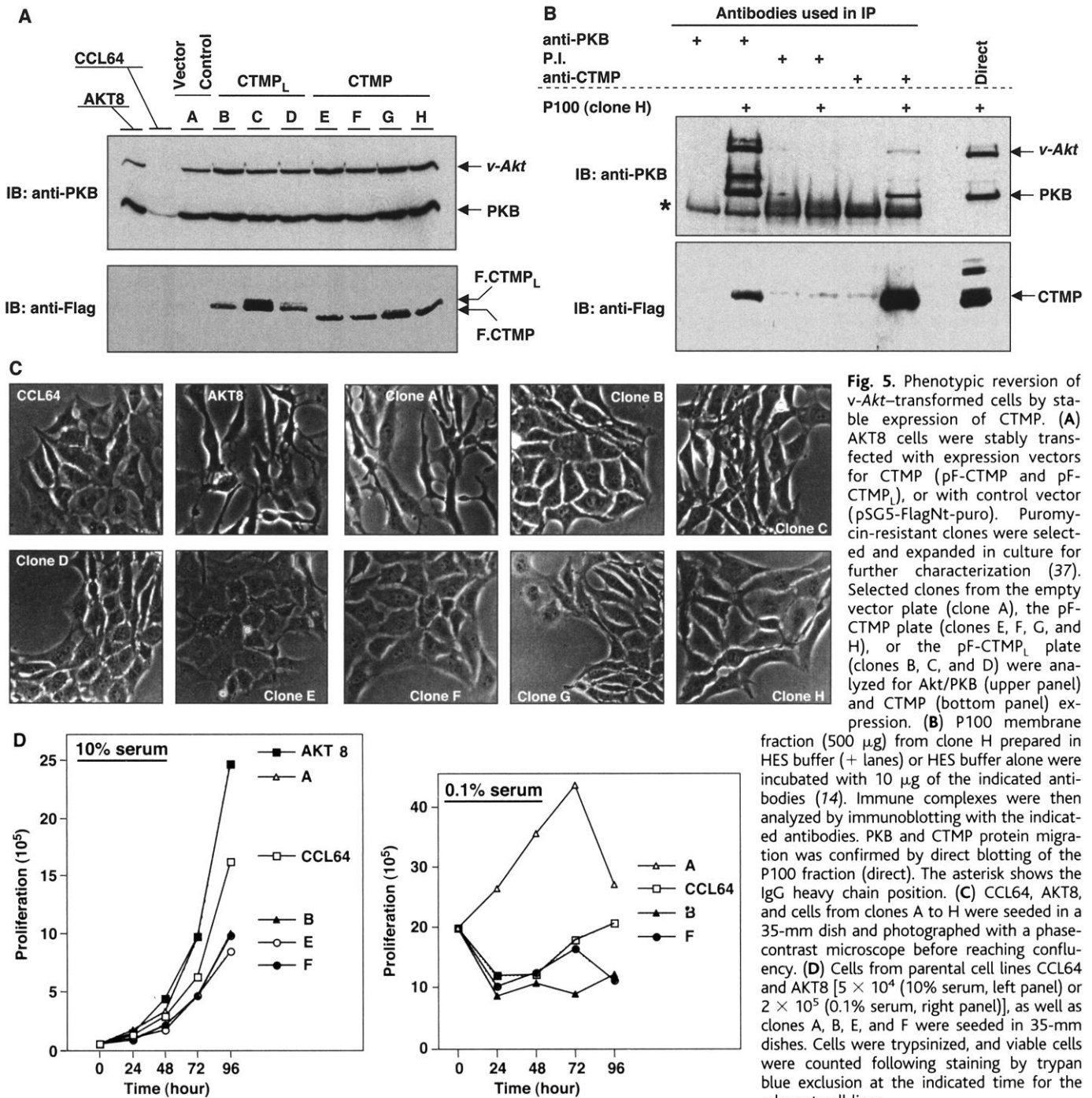


Fig. 5. Phenotypic reversion of *v-Akt*-transformed cells by stable expression of CTMP. **(A)** AKT8 cells were stably transfected with expression vectors for CTMP (pF-CTMP and pF-CTMP_L), or with control vector (pSG5-FlagNt-puro). Puromycin-resistant clones were selected and expanded in culture for further characterization (37). Selected clones from the empty vector plate (clone A), the pF-CTMP plate (clones E, F, G, and H), or the pF-CTMP_L plate (clones B, C, and D) were analyzed for Akt/PKB (upper panel) and CTMP (bottom panel) expression. **(B)** P100 membrane fraction (500 μg) from clone H prepared in HES buffer (+ lanes) or HES buffer alone were incubated with 10 μg of the indicated antibodies (14). Immune complexes were then analyzed by immunoblotting with the indicated antibodies. PKB and CTMP protein migration was confirmed by direct blotting of the P100 fraction (direct). The asterisk shows the IgG heavy chain position. **(C)** CCL64, AKT8, and cells from clones A to H were seeded in a 35-mm dish and photographed with a phase-contrast microscope before reaching confluency. **(D)** Cells from parental cell lines CCL64 and AKT8 [5×10^4 (10% serum, left panel) or 2×10^5 (0.1% serum, right panel)], as well as clones A, B, E, and F were seeded in 35-mm dishes. Cells were trypsinized, and viable cells were counted following staining by trypan blue exclusion at the indicated time for the relevant cell lines.

ation of glycogen synthase kinase-3β (GSK-3β) on Ser⁹, a PKB-mediated phosphorylation event (16).

To determine the consequence of disrupting CTMP function in vivo, HEK293 cells were transfected with an antisense CTMP expression vector (Fig. 4D). Increasing amounts of antisense CTMP cDNA, confirmed by RT-PCR, increased Ser⁴⁷³ phosphorylation of endogenous PKB without changing its expression (Fig. 4D). These data demonstrate that inhibition of endogenous CTMP function increases the activation status of endogenous PKBα and indicate that CTMP acts as a negative regulator of PKBα in

vivo. Supporting these data, similar increases in endogenous GSK-3β phosphorylation on Ser⁹ were also observed in the presence of the antisense CTMP construct, but not a control antisense construct (16). This effect is not due to an up-regulation of PI-3 kinase activity, because no increase in the activity of this enzyme was observed when antisense CTMP or a control luciferase antisense cDNA was expressed (16). Therefore, ablation of CTMP function increases the ability of PKB to activate its downstream effectors in cells.

CCL64 mink lung cells stably expressing *v-Akt* (AKT8 cells), the viral homolog of PKB

isolated from mouse, are transformed and tumorigenic in vitro (19–21). To expand the hypothesis that CTMP negatively regulates PKBα in vivo and to analyze whether CTMP expression could revert the phenotype of *v-Akt*-transformed cells, AKT8 cells were transfected with the cDNA encoding CTMP (CTMP) or with a cDNA corresponding to the original clone isolated from the two-hybrid analysis (CTMP_L). This clone contains an extra 15 amino acids at the NH₂-terminus and was identical to wild-type CTMP in terms of PKBα binding and inhibition (13). Clones stably expressing CTMP were selected and analyzed on the basis of three criteria:

REPORTS

Fig. 6. CTMP inhibits tumor growth in nude mice. AKT8 cells transfected with the puromycin-resistant plasmid (clone A) or stably expressing CTMP (clones B to H) were trypsinized, washed, and resuspended in PBS at a concentration of 10^7 cells/mL. Cells (100 ml , 10^6 cells) were injected subcutaneously into the backs of the nude mice. Three mice were injected for each corresponding cell line. Mice were examined for tumor growth every 3 days. The length and width of each tumor are described at the indicated time after injection.

Clones	Days after injection				
	11	14	20	22	24
CTMP _L A B C D	2.4 × 2.4	3.5 × 4.2	4.8 × 5.8	6.0 × 6.5	8.6 × 10.5
	—	—	—	—	—
	—	—	—	—	—
	—	—	3.2 × 3.2	3.4 × 3.7	4.5 × 4.5
CTMP _S E F G H	—	—	—	—	3.1 × 3.5
	—	—	—	4.2 × 4.2	4.0 × 4.5
	—	—	—	—	—
	—	—	—	—	—

cellular morphology, growth rate, and in vivo tumorigenesis. Expression of CTMP varied somewhat between each cell line (Fig. 5A), whereas amounts of v-Akt remained largely unchanged in all cell lines tested. Significantly, the amounts of endogenous PKB α were increased in v-Akt-transformed cells, a phenomenon not due to cleavage of v-Akt after the Gag NH₂-terminal domain (13). The presence of PKB α -CTMP complexes in vivo was examined by immunoprecipitation using antibodies to either PKB α or CTMP (Fig. 5B). PKB α -CTMP complexes were detected using antibodies to PKB α or Flag, in membrane fractions of clone H (Fig. 5B). Furthermore, v-Akt-CTMP complexes were also detected in this fraction, demonstrating that CTMP interacts with both forms of PKB expressed in these cells, suggesting a conservation of interaction between PKB and CTMP proteins from different species.

Expression of CTMP clearly altered the morphology of AKT8 cells (Fig. 5C); cells were larger in appearance and formed mosaics, similar to wild-type parental CCL64 cells. The change in morphology induced by CTMP expression in these cells may occur via inhibition of v-Akt. In this regard, decreased phosphorylation of v-Akt on Ser⁴⁷³ was observed in cell lines stably expressing CTMP (13). Clones stably transfected with either form of CTMP grew more slowly than did mock-transfected or v-Akt-transformed cells in high serum. Moreover, clones B, E, and F, grew more slowly than untransformed CCL64 cells, suggesting that CTMP inhibited proliferation induced by either v-Akt or by endogenous PKB (Fig. 5D, left panel). In low serum, clones B and F show no significant cell proliferation, which is identical to the profile observed for the parental CCL64 cells (Fig. 5D, right panel). In contrast, AKT8 cells not transfected with the cDNA encoding CTMP (clone A) were still able to proliferate, showing that CTMP expression can restore cell-cycle arrest under low serum conditions.

AKT8 cells form colonies in soft agar (19), suggesting that these cells have tumorigenic properties. We injected nude mice with the different cell lines described in Fig. 5. Mice injected with puromycin-resistant AKT8 cells formed tumors 11 days after injection (clone A, Fig. 6). Tumor growth in these mice was identical to

that in mice injected with AKT8 cells not transfected with CTMP, demonstrating that the presence of the puromycin-resistance gene did not influence tumor growth. Wild-type CCL64 cells did not form tumors when injected into these mice. Analysis of nude mice injected with AKT8 cells stably expressing CTMP revealed that tumor growth was either abolished or delayed to that in animals injected with control AKT8 cells (Fig. 6).

Our results identify CTMP as a new component in the control of PKB α signaling and suggest that this negative regulation, which occurs via a direct interaction of CTMP with PKB at the plasma membrane, may be an important cellular mechanism in preventing inappropriate kinase activation, as well as subsequent excess cell growth and proliferation. The role of PKB in cell survival is well established (2). A key role for PKB in the progression of cancer was illustrated by the discovery of the protein-lipid phosphatase PTEN protein, the most highly mutated tumor-suppressor gene identified since p53 (22, 23). Cells lacking PTEN show increased PKB activity, suggesting that negative regulation of the PI 3-kinase and PKB signaling pathway by PTEN acts to prevent unregulated cell proliferation. Our data demonstrate that CTMP may represent an additional mechanism to negatively regulate PKB in cells. Whereas PTEN inhibits PKB activity indirectly by reducing the amounts of phosphatidylinositol-(3,4,5)-trisphosphate at the cell membrane, CTMP mediates its inhibition by binding directly to PKB and preventing its phosphorylation. In glioblastoma cell lines with compromised PTEN function (U343MG, U87MG), small amounts of CTMP were detected, whereas in glioblastoma cell lines with functional PTEN alleles (LN229), CTMP is readily detected (Fig. 1C). These data suggest that the elevated amounts of PKB activation seen in glioblastoma and other cell lines may be due not just to ablation of PTEN function, but also due to a decrease in the levels of CTMP protein expression in these cells.

References and Notes

1. I. Galetic et al., *Pharmacol. Ther.* **82**, 409 (1999).
2. S. R. Datta, A. Brunet, M. E. Greenberg, *Genes Dev.* **13**, 2905 (1999).

3. D. A. Cross, D. R. Alessi, P. Cohen, M. Andjelkovic, B. A. Hemmings, *Nature* **378**, 785 (1995).
4. M. Andjelkovic et al., *Proc. Natl. Acad. Sci. U.S.A.* **93**, 5699 (1996).
5. D. R. Alessi et al., *EMBO J.* **15**, 6541 (1996).
6. D. R. Alessi et al., *Curr. Biol.* **7**, 261 (1997).
7. D. Stokoe et al., *Science* **277**, 567 (1997).
8. L. Stephens et al., *Science* **279**, 710 (1998).
9. Y. Pekarsky et al., *Proc. Natl. Acad. Sci. U.S.A.* **97**, 3028 (2000).
10. H. Koh et al., *J. Biol. Chem.* **275**, 34451 (2000).
11. Y. Mitsuchi et al., *Oncogene* **18**, 4891 (1999).
12. Supplementary material is available on Science Online at www.sciencemag.org/cgi/content/full/294/5541/374/DC1
13. S.-M. Maira and B. A. Hemmings, unpublished observations.
14. The antibody to Flag was obtained from Sigma, and the phospho-Ser⁴⁷³ and phospho-Thr³⁰⁸ antibodies were from New England Biolabs. The monoclonal antibody (mAb) against HA was from Roche Biomedicals. The polyclonal antibody against PKB was obtained by immunizing rabbits with a peptide corresponding to the last 14 amino acids of PKB α (24). Antibodies against CTMP were obtained by injecting rabbits with bacterially expressed and purified His₆-CTMP protein (99390) or a synthetic peptide corresponding to amino acids 56 to 85 of human CTMP (89570). Affinity purification of immune sera was performed using a protein A-Sepharose column followed by affinity chromatography using recombinant GST-CTMP protein. The P.I. label (Fig. 5B) corresponds to the pre-immune serum from the rabbit before immunization.
15. N. Ishii et al., *Brain Pathol.* **9**, 469. (1999).
16. I. Galetic, B. A. Hemmings, unpublished observations.
17. M. Andjelkovic et al., *J. Biol. Chem.* **272**, 31515 (1997).
18. B. I. Posner et al., *J. Biol. Chem.* **269**, 4596 (1994).
19. S. P. Staal, J. W. Hartley, W. P. Rowe, *Proc. Natl. Acad. Sci. U.S.A.* **74**, 3065 (1977).
20. S. P. Staal, *Proc. Natl. Acad. Sci. U.S.A.* **84**, 5034 (1987).
21. S. P. Staal, J. W. Hartley, *J. Exp. Med.* **167**, 1259 (1988).
22. L. C. Cantley, B. G. Neel, *Proc. Natl. Acad. Sci. U.S.A.* **96**, 4240 (1999).
23. F. Vazquez, W. R. Sellers, *Biochim. Biophys. Acta* **1470**, M21 (2000).
24. P. F. Jones, T. Jakubowicz, B. A. Hemmings, *Cell Regul.* **2**, 1001 (1991).
25. M. Fischer, S. Kaech, D. Knutti, A. Matus, *Neuron* **20**, 847 (1998).
26. B. Chatton, A. Bahr, J. Acker, C. Keding, *Biotechniques* **18**, 142 (1995).
27. C. Chen, H. Okayama, *Mol. Cell. Biol.* **7**, 2745 (1987).
28. M. Andjelkovic, S. M. Maira, P. Cron, P. J. Parker, B. A. Hemmings, *Mol. Cell. Biol.* **19**, 5061 (1999).
29. The cDNA for CTMP obtained from the yeast two-hybrid screen was subcloned into pBluescript KS⁻ (Stratagene). This construct was used as a template for PCR cloning using CTMP-specific primers to generate pGFP-CTMP (in pE-GFP-C1, Clontech), pF-CTMP and pF-CTMP_L (in pSG5-FlagNT-puro, Sigma), or pHook2 (Invitrogen) to allow expression of GFP fusion, Flag-tagged fusion, or untagged CTMP proteins, respectively. The CTMP antisense construct, pAS-CTMP, was generated by cloning the CTMP cDNA in the reverse orientation into the pSG5 vector (Sigma).
30. NIH 3T3 cells were seeded in six-well clusters containing an 18-mm diameter glass coverslip. After transfection, the coverslips were mounted and observed at 37°C as described (25) in observation chambers built for the purpose (Life Imaging Services). Cells were analyzed by using a GFP-optimized filter set (Chroma Technologies). Illumination density was adjusted using neutral density filters and images were taken with a Leica DM-IRBE inverted microscope fitted with an UltraVIEW confocal Live Cell Imaging System (PerkinElmer/Wallac).
31. Indicated cells were lysed in HES buffer (20 mM Hepes-NaOH, pH 7.4, 1 mM EDTA, 250 mM sucrose, 25 mM NaF, 40 mM β -glycerol phosphate,

A Small-Molecule Modulator of Poly- α 2,8-Sialic Acid Expression on Cultured Neurons and Tumor Cells

Lara K. Mahal,¹ Neil W. Charter,² Kiyohiko Angata,⁴ Minoru Fukuda,⁴ Daniel E. Koshland Jr.,² Carolyn R. Bertozzi^{1,2,3*}

Poly- α 2,8-sialic acid (PSA) has been implicated in numerous normal and pathological processes, including development, neuronal plasticity, and tumor metastasis. We report that cell surface PSA expression can be reversibly inhibited by a small molecule, *N*-butanoylmannosamine (ManBut). Inhibition occurs through a metabolic mechanism in which ManBut is converted to unnatural sialic acid derivatives that effectively act as chain terminators during cellular PSA biosynthesis. *N*-Propanoylmannosamine (ManProp), which differs from ManBut by a single methylene group, did not inhibit PSA biosynthesis. Modulation of PSA expression by chemical means has a role complementary to genetic and biochemical approaches in the study of complex PSA-mediated events.

The biological functions of cell surface oligosaccharides have been difficult to elucidate owing to the complexity of achieving genetic control over a molecule that is the product of multiple enzymes and thus of multiple genes. In a few well-studied cases, the function of a specific oligosaccharide epitope has been determined, enhancing our understanding of cell-cell recognition (1). Still, few such structures have been assigned a specific purpose. Small molecules that disrupt or activate a target process in a cellular context have provided insights in systems that are difficult to manipulate with traditional genetic methods (2). The ability to block the expression of a specific oligosaccharide epitope by use of a small molecule would facilitate the study of oligosaccharide function.

PSA (Fig. 1A), a linear homopolymer of α 2,8-linked sialic acid residues, is found mainly on the neural cell adhesion molecule (NCAM) (3, 4). Its biosynthesis is mediated by polysialyltransferases, the best-characterized human homologs of which are ST8SialII (STX) and ST8SialV (PST) (5–7). Both enzymes catalyze the iterative formation of α 2,8-sialic acid linkages using cytidine 5'-monophosphate (CMP)-sialic acid as a substrate. PSA is abundant in the central nervous system during fetal development but is restricted to those regions of the adult brain associated with synaptic plasticity (8–10). In addition, PSA is a marker of several tumors including neuroblastomas, small cell

lung carcinomas, and Wilms tumor (11, 12). It has been implicated in tumor metastasis and the complex neural processes involved in learning and memory (3, 13). We report here a small-molecule modulator of PSA expression.

The cellular machinery for conversion of *N*-acetylmannosamine (ManNAc, Fig. 1B) to CMP-sialic acid tolerates conservatively altered *N*-acyl substituents (14). Thus, administration of *N*-propanoylmannosamine (ManProp, Fig. 1B) or *N*-butanoylmannosamine (ManBut) to cultured cells and laboratory animals results in biosynthesis of the corresponding CMP-sialic acid analogs and the appearance of unnatural sialic acid residues on cell surface glycoproteins. In most sialoglycoconjugates, sialic acid residues occupy terminal α 2,3- or α 2,6-linkages to galactose; replacement of some fraction of these residues with an unnatural variant has no discernible effect on their abundance (15–17). By contrast, in PSA sialic acid occupies both terminal and internal positions, prompting us to consider the effects of incorporation of unnatural sialic acids on its biosynthesis.

We treated NT2 neurons (18) with ManProp or ManBut and visualized PSA expression by immunofluorescence microscopy with the monoclonal antibody (mAb) to PSA 12F8 (19, 20). At concentrations up to 10 mM in the culture medium, ManProp had no effect on PSA expression (Fig. 1C). However, ManBut abrogated 12F8 staining in a dose-dependent manner, indicating that it functions as a metabolic inhibitor of PSA expression (21).

We also analyzed the effects of ManProp and ManBut on the cellular biosynthesis of PSA associated with NCAM. After incubation with various concentrations of ManProp or ManBut, NT2 cells were lysed and subjected to protein immunoblot analysis with the mAb 735 to PSA and the mAb OB11 to NCAM (19). Polysialy-

100 μ M Na₃VO₄, 1 μ M microcystin LR, 1 mM phenylmethylsulfonylfluoride (PMSF), and 1 mM benzamidine) by trituration through a 25-gauge needle 25 times. The nuclei were removed by centrifugation, and the P100 and S100 fractions were obtained by centrifugation at 100 000g for 30 min at 4°C. P100 fractions were resuspended in HES buffer containing 0.1% NP-40, incubated at 4°C for 60 min, and centrifuged at 10000g for 5 min to remove insoluble material. Immunoprecipitations were carried out at 4°C for 2 hours using 5 μ g of antibody to Flag (Sigma) for transfected COS-1 cells, or overnight using 5 μ g of antibody against PKB, or preimmune or antibodies against CTMP for endogenous complexes in untransfected cells. Immune complexes were precipitated using a 1:1 mixture of protein A-protein G-Sepharose (Amersham Pharmacia). The beads were washed, resuspended in 2 \times Laemmli buffer, and analyzed by SDS-PAGE and immunoblotting.

32. The PKB α mAb A4D6 was generated by M. Thelen, P. Cron, A. Wetterwald, and B. A. Hemmings (unpublished results).
33. HA-PKB α and HA-m/p-PKB α expression vectors were described previously (17). pGST-PKB-RD was generated by cloning an Nde I-Eco RI PCR fragment of PKB α into the corresponding sites of the pBC vector (26), referred to as pGST in Fig. 2.
34. Cells were starved for 15 hours in DMEM without serum or phosphate, and then incubated for 4 hours in this medium containing 1 mCi of [³²P]orthophosphate. Cells were then lysed, and Flag-CTMP immunoprecipitated as described (14).
35. Cells were maintained in DMEM supplemented with 10% fetal calf serum (FBS, Life Technologies) and 50 U/ml Pen/Strep (Gibco) for COS-1, HeLa, HEK293, CCL64, AKT8 cells, or 10% calf serum for NIH 3T3 cells. Transfections were performed by using the calcium phosphate technique (27). Transfected COS-1 cells or HEK293 cells were scraped in NP-40 lysis buffer (28), and lysates were cleared by centrifugation at 10 000g for 10 min. HA-PKB α was precipitated with the HA mAb 12CA5 adsorbed to protein A-Sepharose (Amersham Pharmacia). Immune complexes were washed once with lysis buffer containing 500 mM NaCl, once with lysis buffer, and once with 50 mM Tris-HCl (pH 7.8), 1 mM PMSF, 1 mM benzamidine. In vitro kinase assays were as described (28). When required, cells were stimulated with 0.1 mM pervanadate prepared with 0.2 mM H₂O₂ (17).
36. RNA was prepared using the Trizol protocol (Gibco) and reverse transcription reactions were performed using the GeneAmp RNA PCR kit (PE Biosystems). The oligonucleotides T7' and 5'-CTCATCAACTCT-GAACATT-3' were used in RT-PCR reactions to distinguish the antisense construct from the endogenous CTMP cDNA.
37. Four 10-cm dishes of AKT8-transformed CCL64 cells were transfected with 15 μ g pSG5 (negative control), or pSG5-FlagNt-puro (empty vector), pF-CTMP or pF-CTMP_i constructs. After transfection, cells were trypsinized and reseeded in three 10-cm dishes in medium containing 2 μ g/ml puromycin. Colonies were picked after 7 days and grown to confluency in puromycin-containing medium.
38. We thank P. Cron for dedicated technical assistance; J. F. Spetz and P. Kopp for assistance with the nude mice experiments; A. Matus and J. Hagmann for help with confocal microscopy; B. Chatton (IGBMC, Strasbourg, France) for the pBC vector; J. Hartley (NCI, NIH) for the CCL64 and AKT8 cell lines; S. Ruscetti (NCI, NIH) for the antibody against Gag; A. Merlo (Kantonspital, Basel) for the LN229, U343MG, and U87MG glioblastoma cell lines; Y. Nagamine for the p-fos-Luc reporter gene and M. Hill for advice on cell fractionation experiments. S.-M. M. is the recipient of the EMBO long-term post-doctoral fellowship, and part of this work was supported by the Schweizerische Krebsliga (B.A.H.). The Friedrich Miescher Institute is part of the Novartis Research Foundation.

27 April 2001; accepted 22 August 2001

¹Department of Chemistry, ²Department of Molecular and Cell Biology, ³Howard Hughes Medical Institute, University of California, Berkeley, CA 94720, USA. ⁴Glycobiology Program, Cancer Research Center, Burnham Institute, La Jolla, CA 92037, USA.

*To whom correspondence should be addressed. E-mail: bertozzi@cchem.berkeley.edu